

Probing the Molecular Structure and Bonding of the Surface of Aqueous Salt Solutions

Elizabeth A. Raymond and Geraldine L. Richmond*

Materials Science Institute and Department of Chemistry, University of Oregon, Eugene, Oregon 97403

Received: December 5, 2003; In Final Form: February 5, 2004

The surfaces of aqueous solutions of NaF, NaCl, NaBr, and NaI have been examined using vibrational sum-frequency spectroscopy. Spectra of these salts in mixtures of HOD/H₂O/D₂O have been used to provide insight into how simple salts alter the hydrogen bonding structure of water in the surface region. As the anion is changed, the observed interfacial hydrogen bonding also changes, indicating the presence of anions in the interfacial region. The isotopic dilution experiments performed on each solution enable separation of the contributions arising from interfacial water with differing degrees of hydrogen bonding. Frequency shifts in the peaks attributed to tetrahedrally coordinated water molecules within the interfacial region display the structure-making characteristics of F⁻ and the structure-breaking characteristics of Cl⁻, Br⁻, and I⁻. However, water molecules residing in the topmost surface layer show minimal perturbation by the presence of these anions as probed by the characteristics of the donor OH mode of water molecules that straddle the air/water interface. These results indicate a significantly diminished population of the anions at the uppermost layer of the surface region.

Introduction

For the past several decades, the prevailing view of the surface of aqueous salt solutions is that it is largely devoid of ions.¹ This picture has been based largely on macroscopic thermodynamic measurements such as surface tension. Recently this view has been called into question by a series of experiments^{2–4} and molecular dynamics simulations^{5–8} that show preferential adsorption of the more polarizable anions to the surface region over that of the smaller, less polarizable cations. What has been lacking in the development of a more complete understanding of these surfaces is direct measurement of the effect of ions on the surface bonding interactions occurring in these salt solutions. Because surface tension is ultimately related to bonding and structuring of the interfacial water molecules, the measurement of how the presence of salt alters the surface hydrogen bonding is critical to understanding this puzzle.

In addition to being a system of atmospheric relevance,^{3,9–11} the effect of simple ions on the vapor/water interface is of general thermodynamic interest. Most simple ions are ranked (via the Hofmeister series) on the basis of their effect on the surrounding water structure.^{12,13} This method of organizing ions based upon their abilities to create or destroy structure in the surrounding water network is of particular use when studying proteins in aqueous solutions.¹³

Vibrational sum-frequency spectroscopy (VSFS) has been used to measure changes in the hydrogen bonding of water in the interfacial region as a result of the presence of simple electrolytes in the solution. Previous VSFS studies have demonstrated how valuable such measurements can be in measuring the hydrogen bonding of water molecules at this surface and the sensitivity of the OH stretching modes of water in the presence of adsorbed surface species.^{14–16} Isotopic dilution experiments have been particularly powerful in the identification of specific interfacial water species with different bonding

character.^{17,18} Such studies of the vapor/H₂O/HOD/D₂O interfaces are ideally suited for deconvolving complicated H₂O spectral features by taking advantage of the energetically uncoupled nature of the OH and OD stretching modes in HOD. In particular, such experiments allow the direct measurement of the frequency and bandwidth of the “donor” OH bond of the water molecules that straddle the vapor/water interface. This donor mode, which is directed into the liquid phase and is vibrationally uncoupled from its adjacent free OH mode that is directed into the air, has been shown to be highly sensitive to the water bonding environment in the topmost surface layer.^{17–19} Isotopic dilution experiments allow measurements of the frequency and bandwidth of this mode directly, a feat that is otherwise impossible for H₂O solutions because of overlapping adjacent OH bands.

The studies presented here employ VSFS isotopic dilution experiments to examine the effect of simple alkali halide salts on the interfacial water structure. For simplicity, the cation (Na⁺) has been held constant while the anion has been changed from the small, relatively unpolarizable F⁻ to the progressively larger, more polarizable Cl⁻, Br⁻, and I⁻. By changing only the anion, the effect of anion size and polarizability on the surface hydrogen-bonding network can be isolated. The alkali cations are quite small, are relatively unpolarizable, and have a much smaller effect on the water structure than the anion.^{12,13} The results demonstrate that for the four alkali halide salt solutions studied—NaF, NaCl, NaBr, and NaI—the interfacial hydrogen bonding between water molecules is altered by the presence of salt and the changes are dependent on the identity of the anion. However, the bonding interactions in the topmost boundary layer are found to be negligibly affected by the presence of the ions.

Thermodynamic Discussion

The surface tension of a neat vapor/water interface is reduced by the addition of most molecules. Exceptions to this general rule are simple electrolytes, which increase the surface tension of the vapor/solution interface relative to that of a neat interface.

* To whom all correspondence should be addressed. E-mail: richmond@darkwing.uoregon.edu.

This behavior has been known since ca. 1910²⁰ and has been the subject of considerable study, both experimental and theoretical. Changes in surface tension can be related to the composition of the interfacial region using the Gibbs equation and the concept of Gibbs surface excess.¹ Within this treatment, the interfacial region is defined as the region in which the number of molecules of solute per unit volume (the concentration) differs from that of the bulk. The difference between the bulk and interfacial concentrations, the surface excess (Γ), is related to the change in surface tension (γ) as a function of concentration (c) by eq 1.¹

$$\Gamma = -\frac{1}{RT} \left(\frac{d\gamma}{d \ln c} \right) \quad (1)$$

This surface excess can be either positive, when there is a higher interfacial concentration of solute (as with conventional surface active molecules), or negative, when the interfacial concentration is smaller than the bulk concentration (which is the case for the salts discussed in these studies). It is this reduced interfacial concentration of ions that is often interpreted as a lack of ions at the vapor/water interface.

These thermodynamic arguments, however, contain no molecularly specific information about the structure of the interfacial region, nor do they discuss the types of molecular interactions responsible for this partitioning of species. The 1934 model of Onsager and Samaras used the concept of image charges (originally proposed by Wagner²¹) to explain the increase in surface tension of simple electrolyte solutions.²⁰ Although this model predicts surface tensions reasonably well at low concentrations, it does not predict the linear increases in surface tension that continue up to high concentrations,^{12,22} nor does it explain the differences in surface potential measured for different electrolyte solutions.^{23,24} The model assumes that both anions and cations are repelled equally from the interface (thereby producing no surface potential) and that a layer of water exists at the surface that is completely devoid of ions. Experimental surface potential measurements of NaCl, NaBr, and NaI solutions see increasingly negative surface potentials with increasing anion size, implying that the anions are closer to the surface than the cations.^{12,23,24}

Over the past 70 years, there have been many attempts to develop a model which correctly predicts the surface tensions and surface potentials of simple electrolyte solutions. Several of the recent models have included properties of the specific anions and cations as well as interactions between the ions and the surrounding water molecules that improve the agreement with experimental data but are still not entirely satisfactory.^{22–24} This lack of a clear molecular-level model that correctly reproduces the experimentally obtained surface tension and surface potential measurements illustrates the need for experimental data that directly probes the interfacial region.

VSFS Background

VSFS provides vibrational spectra of molecules at the interface between two media that are perturbed by the presence of that interface. In the case of the vapor/water interface, probing these molecules in the OH stretching region provides a picture of the interfacial hydrogen-bonding interactions. The VSFS intensity measured as a function of frequency is proportional to the intensity of the visible and tunable infrared beams incident upon the interface. The intensity is also proportional to the square of the nonlinear susceptibility. In interpreting VSFS

spectra, it is important to recognize that this nonlinear susceptibility, $\chi^{(2)}$, can be decomposed into two pieces, a nonresonant and a resonant component. The measured intensity is represented by eq 2, where I_{vis} and I_{IR} represent the incident intensities of the visible and tunable infrared beams, respectively.

$$I_{\text{SF}} \propto |\chi_{\text{NR}}^{(2)} + \sum_{\nu} \chi_{\nu}^{(2)}|^2 I_{\text{vis}} I_{\text{IR}} \quad (2)$$

The nonresonant susceptibility, $\chi_{\text{NR}}^{(2)}$, is constant as a function of frequency for the vapor/water interface, while the resonant susceptibility is composed of a sum of resonant peaks, $\chi_{\nu}^{(2)}$, with each peak representing a distinct molecular species. Because each of these susceptibility terms is a complex quantity having both an amplitude and a phase and the contribution to the intensity from the nonlinear susceptibility arises from the square of a sum of terms, interferences are expected to arise between the individual components. For further details of VSFS, readers are referred to refs 15, 16, 18, 25, and 26.

Experimental Details

The salts used were purchased from Sigma-Aldrich (ACS reagent grade, 99%+ purity) and were kept sealed and used as received. All H₂O solutions were made with water from a Millipore Nanopure system, (resistivity >17.8 MΩ cm), and the D₂O solutions were prepared with 99.9% D₂O obtained from Cambridge Isotopes. Two equal-concentration solutions were made of each salt, one in H₂O and one in D₂O. Quantities of each solution (measured by weight in Gastight syringes) were mixed directly in the sample dish within the cell under flowing N₂(g). Preparing isotopic mixtures in this way ensures a constant salt concentration while allowing variation of the H₂O and D₂O concentrations from 0 to 100%. The salt concentration of the NaCl, NaBr, and NaI solutions was 0.030 mf (mole fraction) and that of the NaF solutions was 0.016 mf due to the lower solubility of NaF. It is important to note that at these high ionic strengths (0.03 mf ≈ 1.7 M) the double-layer thickness expected from Gouy–Chapman theory is very small, ~2.7 Å.¹ Because of measurement by mass (rather than volume) and the use of mole fraction, calculation of the equilibrium concentrations of H₂O, HOD, and D₂O in each sample does not require knowledge of solution densities or partial molar volumes of the salts.

To prolong the life of the aqueous NaI solutions, which are light-sensitive, the solution containers were masked with tape to create a dark environment. Care was also taken to minimize the exposure of the solutions to light (i.e., room lights were dimmed while solutions were made as well as during transfer into the experimental sample cell).

The laser system used in these experiments has been extensively described in previous publications, so a description is not provided here.^{18,27,28} The presented spectra were taken under SSP polarization conditions. SSP polarization conditions probe molecules with components of their dipole moment perpendicular to the interfacial plane and components of their Raman moment parallel to the interfacial plane. All spectra were taken with 2-s exposures of a thermoelectrically cooled CCD camera, and two to four spectra were averaged to obtain the spectra shown. The spectra have been normalized by the SF spectrum of Au (which is purely nonresonant in this spectral region) to remove the dependence on the incident visible and IR intensities as well as other experimental artifacts;¹⁸ therefore,

they are proportional only to the square of the nonlinear susceptibility, $|\chi_{\text{NR}}^{(2)} + \sum_v \chi_v^{(2)}|^2$. The spectra are all scaled relative to neat H₂O spectra taken on each day so that spectral intensities may be directly compared.

Spectral analysis procedures used in this study are similar to that described in our previous publications for neat water surfaces.^{17,18} One difference for these salt solutions is that the spectra have not been normalized by the Fresnel coefficients. The fitting analysis has been re-performed on the isotopic dilution series for the pure vapor/water interface, and although some peak parameters changed slightly, the conclusions did not change. This analysis was performed again so that the salt solution spectra could be directly compared to that of the neat interface, as the Fresnel coefficients could not be directly calculated for the salt solution spectra due to the unavailability of the indices of refraction as a function of wavelength.

The fitting routine used for each isotopic dilution series is performed iteratively such that the peak frequency, width, and phase obtained for each resonant peak are global parameters for each individual salt solution, independent of H₂O/HOD/D₂O concentrations. Fitting the spectra in this manner constrains the fits, leaving only the peak amplitudes as truly free parameters, thereby enabling the spectra to be fit with confidence.

Results

Before discussing how the interfacial hydrogen bonding is changed upon the addition of salts, a brief review of what is known about the pure vapor/water interface is warranted. Previous isotopic dilution VSFS experiments^{17,18} have enabled the relatively broad OH stretching region of hydrogen-bonded surface water molecules to be separated into distinct spectral peaks arising from various contributing surface water species. The VSFS response from the neat vapor/water interface consists of four resonant features as well as a nonresonant response (obtained from a vapor/D₂O spectrum). The four resonant peaks are assigned to the OH stretching of two distinct types of water molecules. The highest-energy peaks correspond to water molecules that straddle the interface such that one OH oscillator protrudes into the vapor and participates in minimal hydrogen bonding (free OH), whereas its adjacent OH oscillator (donor OH) points on average toward the bulk liquid and participates in hydrogen bonding interactions characteristic of those found in bulk liquid water. Because of the large difference in hydrogen bonding between the free and donor OHs, the two vibrations are nearly uncoupled, as evidenced by a separation in frequency of approximately 250 cm⁻¹. The other type of interfacial species contributing to the vapor/water spectrum is water molecules that participate in more highly coordinated hydrogen bonding. Though these species are completely surrounded by other water molecules, their contribution to the VSFS spectra indicates that they are still influenced by the presence of the interface. Two spectral peaks have been assigned to these types of molecules, both of which are consistent with the spectral intensity observed in IR and Raman studies of bulk liquid water. For simplicity, the bonding of these molecules is referred to as tetrahedral, though every molecule is likely not fully symmetrically tetrahedrally bonded.

Figure 1a shows the VSFS spectrum of the neat vapor/water interface and its corresponding fit as derived from isotopic dilution experiments. Figure 1b shows the fit with the nonresonant component removed and its composite peaks. The peaks at 3705 and 3454 cm⁻¹ are assigned to the free and donor OH vibrations, respectively, whereas the peaks at ~3200 cm⁻¹

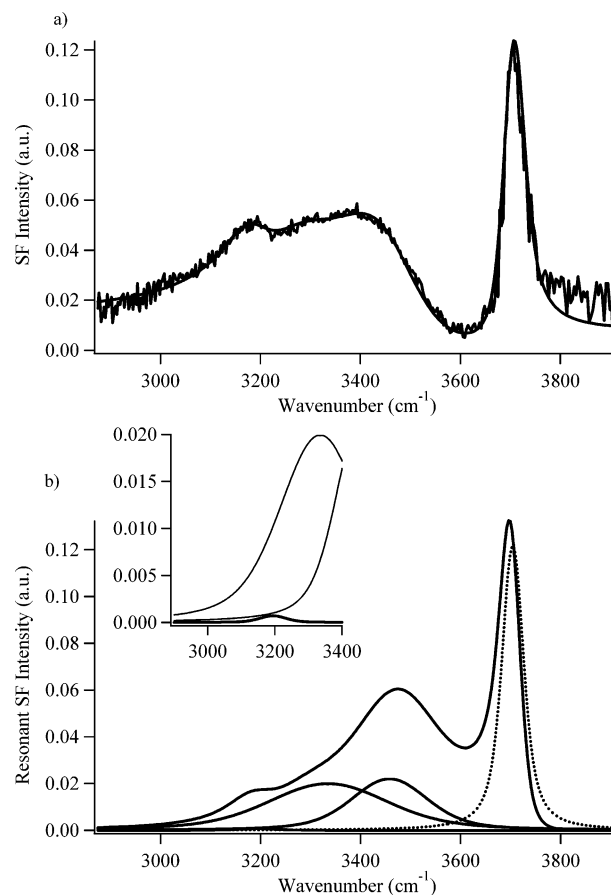


Figure 1. (a) VSF spectrum of the vapor/water interface taken under SSP polarization conditions. The smooth line is the best fit to the data. (b) Fit to the vapor/water spectrum with the nonresonant component removed. Also shown are the composite resonant peaks where the dotted line is π out of phase with the solid-line peaks. The inset shows the 3200-cm⁻¹ peak more clearly.

(shown as an inset for clarity) and 3325 cm⁻¹ are assigned to vibrations of the tetrahedrally coordinated interfacial water molecules. The phase of the free OH is chosen to be 0, whereas the phases of the other three resonant features and the nonresonant feature are π .^{17,18} The average peak frequencies and widths are included with the parameters of the salt-containing solutions in Table 1.

Figure 2 shows the SF spectra of NaF, NaCl, NaBr, and NaI, with neat vapor/water spectra overlaid for comparison. The aqueous NaF spectrum shows a decreased intensity relative to that of neat water in the 3150–3500-cm⁻¹ region, unlike the other three salt solution spectra. This decrease in intensity in the central region is the largest difference between the NaF solution and neat water spectra. Careful inspection of the free OH peak shows a slight intensity increase on both sides of the peak. The spectra of 0.03 mol fraction (mf) NaCl is very similar to the neat water spectrum, with slight increases in intensity in the 3300–3400 and 3800 cm⁻¹ regions. These increases become more pronounced in the NaBr and NaI spectra, following the trend of increasing anion size, with the NaI solution having the largest intensity. The intensity of the low-frequency end of the NaI solution is significantly lower than that of neat water, unlike the other three salt solution spectra, where the intensity is very similar to that of the water spectrum. A more subtle feature develops as the anion size is increased, in the intensity well around 3600 cm⁻¹. As the anion size increases, this well becomes less symmetric, with a deepening on the low-energy side.

TABLE 1: Average Frequencies and Widths for the Resonant Peaks Obtained from the Neat H₂O and Aqueous Salt Solution Spectra with Their Corresponding Uncertainties^a

	tetrahedral		tetrahedral		donor OH		free OH		solvation		solvation	
	ω_v	Γ_v	ω_v	Γ_v	ω_v	Γ_v	ω_v	Γ_v	ω_v	Γ_v	ω_v	Γ_v
NaF	3212 ± 7	32 ± 7	3285 ± 7	230 ± 15	3445 ± 7	110 ± 10	3701 ± 5	16 ± 4	3625 ± 7	85 ± 12	3760 ± 10	85 ± 10
H ₂ O	3195 ± 7	42 ± 7	3325 ± 10	133 ± 10	3454 ± 8	92 ± 10	3705 ± 5	19 ± 4				
NaCl	3210 ± 7	27 ± 7	3335 ± 7	130 ± 10	3454 ± 7	93 ± 10	3705 ± 5	16 ± 4	3647 ± 7	35 ± 5	3750 ± 7	85 ± 10
NaBr	3212 ± 7	30 ± 7	3350 ± 7	105 ± 10	3461 ± 7	90 ± 10	3705 ± 5	16 ± 4	3645 ± 7	33 ± 5	3760 ± 7	85 ± 10
NaI	3207 ± 7	45 ± 7	3360 ± 7	110 ± 10	3478 ± 7	78 ± 10	3701 ± 5	20 ± 4	3632 ± 7	57 ± 6	3770 ± 7	96 ± 10

^a All values are given in units of cm⁻¹

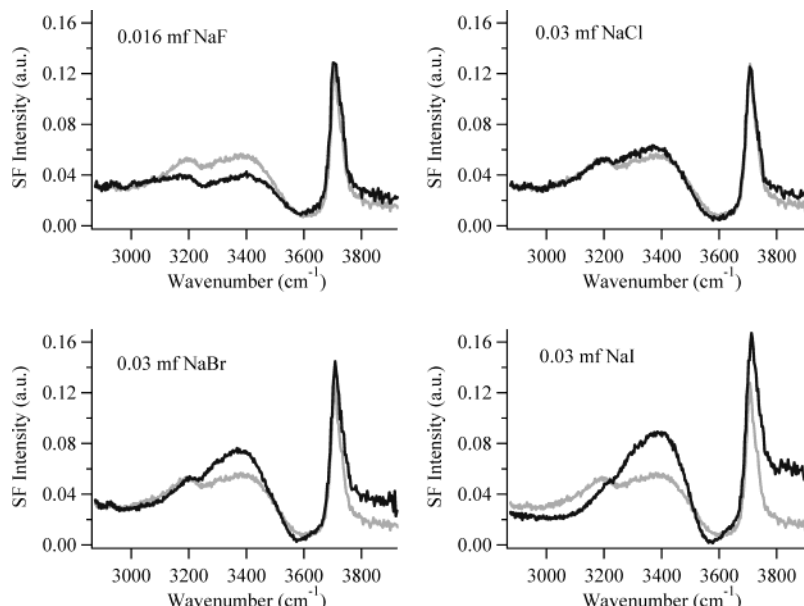


Figure 2. VSF spectra of 0.016 mf NaF, 0.03 mf NaCl, 0.03 mf NaBr, and 0.03 mf NaI in H₂O (black). A neat vapor/water spectrum (grey) is shown with each salt solution spectrum for comparison.

In the visual comparison of the spectral changes in the broad OH-bonded region for the different salts, the intensity changes and frequency shifts for F⁻ relative to those of the other more polarizable anions could be due to a reorientation of the surface water molecules as the halide ion is changed, or the increase in intensity with increasingly polarizable anion is indicative of a higher concentration in the surface region. Although such arguments are plausible, qualitative interpretation based on simple inspection is neither unique nor rigorous. Creating a molecular-level description of the hydrogen bonding environment of surface water molecules based on VSF spectra requires performing isotopic dilution experiments on these four salt solutions so that the resonant and nonresonant features can be characterized and separated. As mentioned previously, these isotopic dilution experiments not only reduce the number of contributing interfacial species (for solutions with very low H₂O content) but also provide constraints on the spectral fitting parameters for each series through the use of a global fitting routine.

VSF measurements of salts in D₂O provide information about the magnitude of the nonresonant VSF response from the vapor/water interface. These spectra are flat in the OH stretching region, which is indicative of a purely nonresonant SF response. However, the intensity increases from that observed for pure D₂O upon the addition of salt as well as when the anion is changed. Figure 3 shows the magnitude of the nonresonant susceptibility, | χ_{NR} |, for neat D₂O as well as the NaF, NaCl, NaBr, and NaI solutions, and the values are given in Table 2. Recall that the observed spectral intensity is proportional to the square of this magnitude. The nonresonant magnitude is

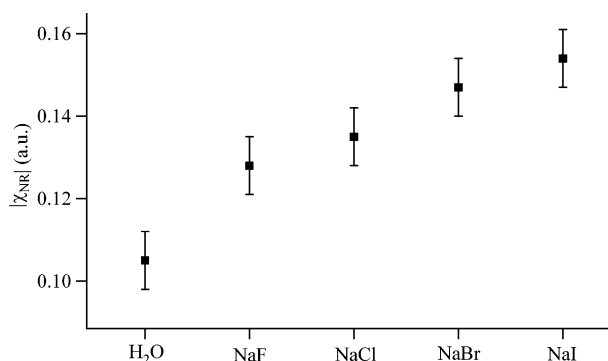


Figure 3. Magnitude of the nonresonant response in the OH stretching region for pure D₂O and the four salts in D₂O.

TABLE 2: Magnitude of the Nonresonant Response in the OH Stretching Region for Pure D₂O and the Four Salts in D₂O

	$\chi_{NR}^{(2)}$ (au)
D ₂ O	0.105 ± 0.007
NaF	0.128 ± 0.007
NaCl	0.135 ± 0.007
NaBr	0.147 ± 0.007
NaI	0.154 ± 0.007

proportional to the number of contributing molecules as well as the polarizability. Thus, the observed increases can be attributed to a larger number of contributing water molecules, implying that the interfacial region is thicker, or an increase in the polarizability of the interfacial region either from the increasing polarizability of the ions or an enhancement in the

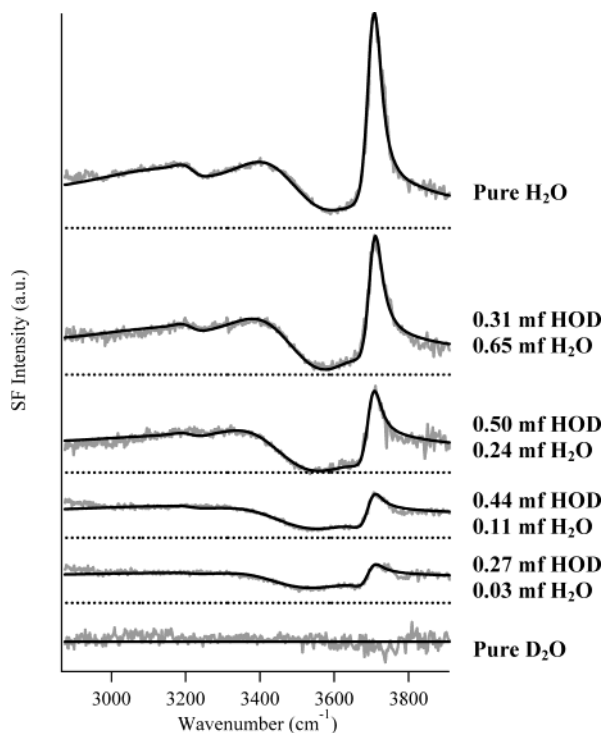


Figure 4. VSF spectra (grey) of the isotopic dilution series of 0.016 mf NaF with the best spectral fits (black). Isotopic concentrations are included on the right. The spectra have been offset, and the dotted lines represent the zero of intensity for each spectrum.

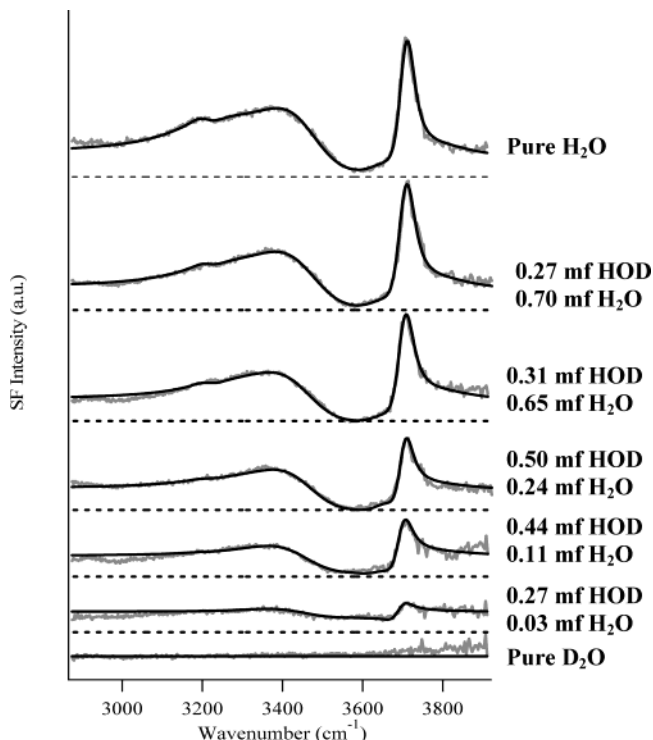


Figure 5. VSF spectra (grey) of the isotopic dilution series of 0.03 mf NaCl with the best spectral fits (black). Isotopic concentrations are included on the right. The spectra have been offset, and the dotted lines represent the zero of intensity for each spectrum.

water polarizability arising from ion–water interactions. All three arguments are possible and, unfortunately, experimentally indistinguishable.

By holding the concentration of salt in each solution constant while changing the concentration of H₂O, D₂O, and HOD and using an iterative global fitting routine (as was done in studies

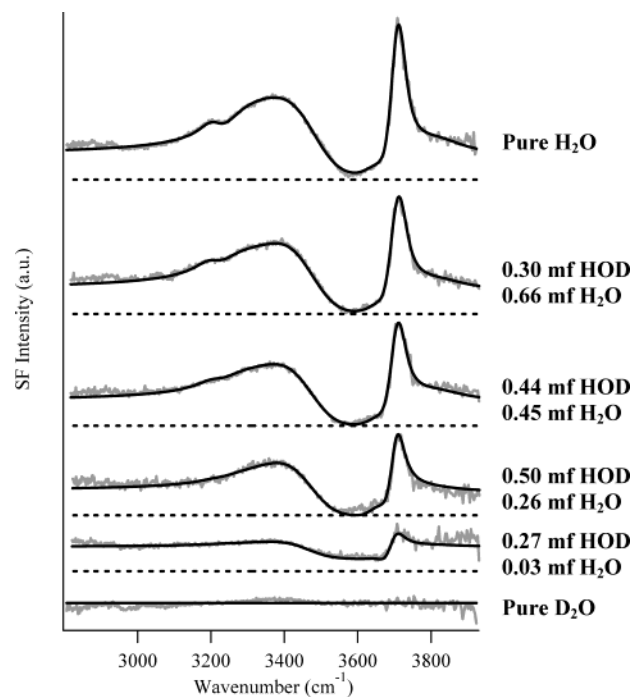


Figure 6. VSF spectra (grey) of the isotopic dilution series of 0.03 mf NaBr with the best spectral fits (black). Isotopic concentrations are included on the right. The spectra have been offset, and the dotted lines represent the zero of intensity for each spectrum.

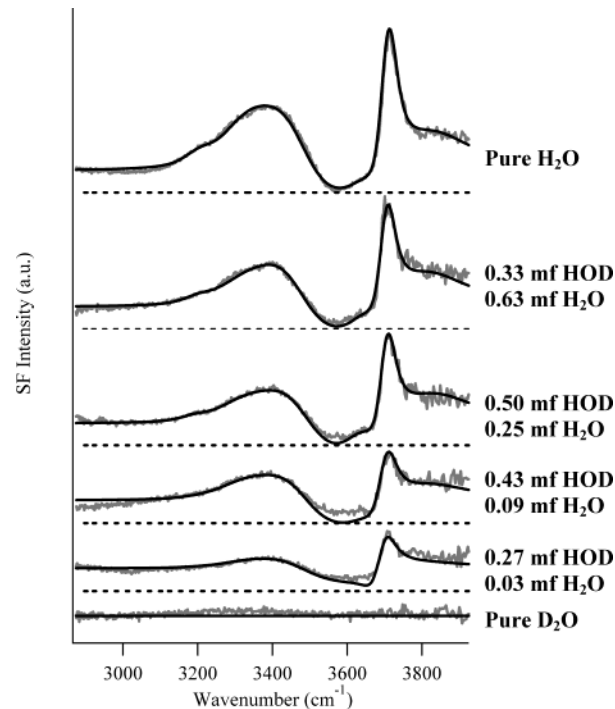


Figure 7. VSF spectra (grey) of the isotopic dilution series of 0.03 mf NaI with the best spectral fits (black) as described in the text. Isotopic concentrations are included on the right. The spectra have been offset, and the dotted lines represent the zero of intensity for each spectrum.

of the neat H₂O interface^{17,18}), the resulting spectra can be decomposed into their composite spectral features. The resulting spectra and their best fits are shown in Figures 4–7. Each of these spectral series was fit with six resonant peaks and the nonresonant amplitudes obtained from the salt-containing D₂O spectra. (See Table 2.) With the exception of the NaI solutions (which will be discussed later), all phases were constrained to

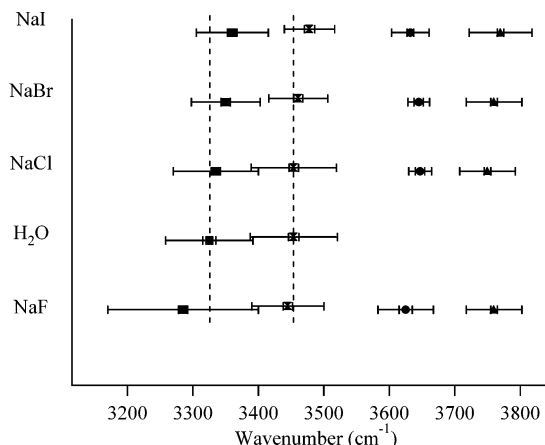


Figure 8. Trends in peak frequency and width for neat H_2O and the four salt solutions. The marker represents the average center frequency, the narrow error bars represent the uncertainty in frequency, and the large error bars represent the peak width. The dashed line facilitates comparison with the neat water values.

0 or π and are the same as those obtained from the pure H_2O series. Four of the resonant peaks have the same assignments as those in the pure H_2O series: two tetrahedrally coordinated water peaks and the donor and free OH peaks. In addition to these four peaks, two additional peaks were added, one on each side of the free OH, which are attributed to the OH stretching of water molecules solvating the ions in the interfacial region. The phases of these two peaks are the same as that of the free OH, indicating an average molecular orientation with the hydrogens pointing away from the bulk liquid.

The agreement of the fits with the experimental data for the NaF (Figure 4), NaCl (Figure 5), and NaBr (Figure 6) series is excellent, capturing the spectral shape of the broad peak, the intensity well around 3600 cm^{-1} , the free OH peak, and even the high-energy tail of the free OH, whose intensity increases as the anion size increases.

For the NaI spectral series (Figure 7), the fits are good except for in the region of the intensity well around 3600 cm^{-1} in the lowest-concentration H_2O solutions. After an exhaustive examination of optimum fitting parameters in the global fits, it was determined that the best fit (shown in Figure 7) in this region could be obtained only if the phases of the two tetrahedrally bonded peaks were allowed to vary. Allowing these parameters to vary in the global fit of the entire NaI isotopic dilution series, we determined the resulting phase of these peaks to be $2 \pm 0.1 \text{ rad}$, ($\sim 115 \pm 5^\circ$). That these peaks remain out of phase with the free OH suggests a minimal change in the orientation of the tetrahedrally bonded water molecules with the addition of I^- . Further assignment of a more specific orientation to this new phase is complicated because this one phase angle is related to three orientation (Euler) angles, as well as the symmetry of the vibrational mode being probed.^{29–31} Allowing the phase of the tetrahedral peaks to vary in the NaF, NaCl, and NaBr spectral fitting did not result in significant improvement of the fits, nor was it physically insightful.

Discussion

The isotopic dilution experiments of Figures 4–7 and the application of a global fitting routine to the data sets for each type of salt solution allow the otherwise broad OH stretching peak for the surface hydrogen-bonded water molecules to be deconvolved into contributing water species. Figure 8 shows the peak frequencies (marker), uncertainties (narrow error bars), and widths (wide error bars) for the large tetrahedral, donor

OH, and solvation peaks for all four salt solutions as well as the values from the neat water interface. The small tetrahedrally bonded peak ($\sim 3200 \text{ cm}^{-1}$) and the free OH peak remain constant in both frequency and width for the different salt solutions and so are not shown in Figure 8. The constant nature of the free OH peak (in pure H_2O solutions) is consistent with the non-hydrogen-bonding nature of the free OH oscillator. The frequency of this vibration is again evidence of its minimal hydrogen bonding and almost complete uncoupling.

The large tetrahedrally bonded peak undergoes large frequency shifts depending on the composition of the solution. In the NaF solution, the peak is considerably red shifted from the frequency observed in neat H_2O and is also significantly broader. Such spectral changes are consistent with the presence of the fluoride ion, causing a strengthening of interactions between surface water molecules. The fluoride ion containing solutions exhibit the type of “structure-making” properties in the surface region as have been observed in IR and Raman studies of bulk NaF solutions.^{12,32}

The frequency of the larger tetrahedrally bonded water peak in the NaCl solutions is slightly blue shifted from that of neat water, but the difference is within the experimental error. The width of this peak is very similar to that from the neat H_2O spectrum. Bulk studies of NaCl in H_2O show a slight blue shift and a narrowing of the OH stretching features.^{12,32,33} Cl^- is considered to be a structure-breaking ion, but less so than Br^- or I^- . The large tetrahedral peak in the NaBr solution shows a more significant shift to higher energy and is also narrower than that observed in liquid H_2O . This larger shift agrees well with the greater “structure-breaking” nature of Br^- .¹² Both the blue shift and the narrowing are consistent with bulk studies of NaBr in H_2O .^{12,32,33} The tetrahedral peak of the NaI solutions, in addition to changing phase, as mentioned above, has also shifted the farthest to higher energy (of the anions studied here, I^- is ranked the highest in its structure-breaking abilities) and is similar in width to the peak in the NaBr solution spectrum. Again, this frequency shift is in agreement with bulk studies, though most studies have seen the OH stretching features be the narrowest for NaI solutions.^{12,32–34} The VSF results for these three anions clearly indicate that they are present in the surface region and that their structure-breaking effect is similar in the surface region to what is observed in the bulk.

The donor OH peak frequencies and widths exhibit minimal change with changing solution composition, in contrast to what is observed for the tetrahedrally bonded OH peak. The widths and frequencies for the neat H_2O , NaF, NaCl, and NaBr solutions are all within experimental error of each other. For NaI-containing solutions, the donor OH peak appears to shift slightly to higher energy and is slightly narrower than the donor OH of the other solutions.

The observed near constancy in the peak frequency and peak widths for the donor OH modes for these halide-containing solutions differs significantly with what is observed in bulk spectroscopic studies of salts in deuterated water. Measurable frequency shifts and bandwidth changes of the donor mode are observed in bulk IR studies of HOD in corresponding salt solutions in D_2O .^{12,33,35} Similar spectral changes in the donor mode have also been obtained in IR studies of water clusters with attached anions.^{36,37} The results of these previous bulk HOD studies are consistent with the structure-making and structure-breaking behavior found in the bulk IR and Raman data of the salts in H_2O . They are not, however, consistent with our SF measurements. That the donor OH peak in the salt solutions is not changing significantly (relative to that of neat

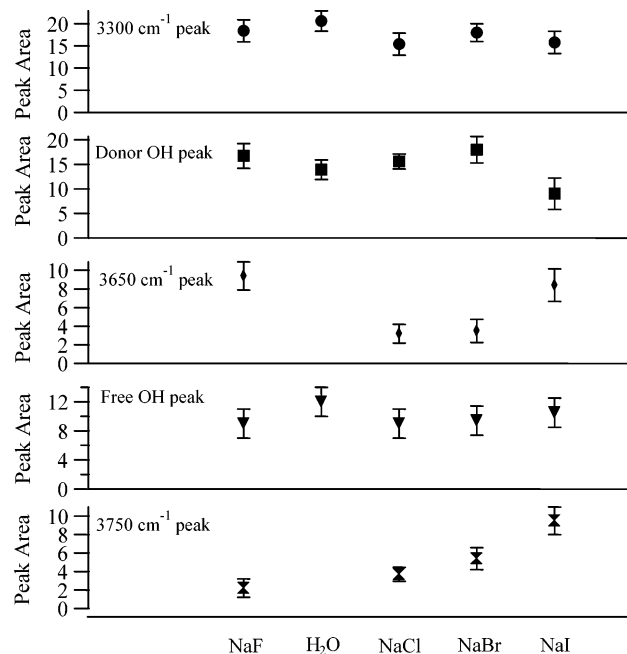


Figure 9. Peak areas of the resonant features for neat H_2O and the four salt solution spectra. Error bars represent the uncertainty in the areas.

water) signifies that either the ion concentration is negligible or that any nearby ions have a minimal effect on the bonding in the topmost surface layer (where the donor OH oscillators reside). The small change associated with the NaI solution may indicate that the concentration of I^- in the top surface layer is higher than that of the other ions or may be indicative of the stronger effect that I^- appears to have on the water bonding network.

The two remaining small resonant peaks in the spectral fits are assigned to the OH stretching of water molecules in the interfacial region that are in close proximity to the ions. Recall that these species are not present in the pure vapor/water spectrum. The high frequencies of these solvating peaks indicate that these molecules are participating in weak hydrogen bonding. Peaks with similar frequency and phase characteristics have been found in VSF studies of ions at the $\text{CCl}_4/\text{H}_2\text{O}$ interface and have been attributed to solvating ions that become oriented because of ion–dipole interactions.³⁸ Studies of ions in small water clusters also show spectral features in this region.³⁹ With the exception of the lower-energy peak in the NaF solution, the areas of the two solvation peaks (which are obtained by multiplying the peak amplitude A_v by the width Γ_v ; see ref 18 for details) increase with increasing anion size. (See Figure 9.) The progressively increasing contributions from these weakly bonded water molecules create the observed asymmetry in the intensity well at $\sim 3570 \text{ cm}^{-1}$, and the large intensity increases to the blue of the free OH. This increase in the peak areas with increasing anion size further indicates that these peaks are arising from water molecules solvating interfacial ions. The larger area is caused by either a greater number of contributing molecules or increased signal per molecule arising from the ion–water interactions. As with the nonresonant response increase, these two effects are experimentally indistinguishable.

Figure 9 also shows the areas of the other resonant peaks for each of the salts in pure H_2O , as well as the areas from the neat H_2O spectrum, for comparison. The areas for the small tetrahedrally coordinated peak ($\sim 3200 \text{ cm}^{-1}$) are not shown as they are quite small and constant from solution to solution (well within experimental uncertainties).

One of the most interesting results from this analysis is that the peak areas of the large tetrahedrally coordinated ($\sim 3300 \text{ cm}^{-1}$), donor OH, and free OH peaks remain constant as the solution composition is changed. The one exception to this is the slight decrease in the donor OH area of the NaI solution, though this may be related to the uncertainty in the spectral phase change for the two tetrahedral peaks. The constant peak areas are particularly interesting given that simple inspection of Figure 2 might suggest that the overall intensity grows with increased anion polarizability. The discrepancy between the interpretation derived from simple inspection and the detailed analysis presents a clear example of why accurate molecular interpretations require careful analysis of VSF spectra. The observed decrease in intensity (relative to the intensity in neat water) in the NaF solution spectrum (Figure 2) arises from the distribution of intensity over a much broader region, centered at lower energy. In the NaCl, NaBr, and NaI solutions, the increased intensity in the 3400 cm^{-1} region (relative to the intensity in neat water) is due to narrowing of the spectral intensity from the tetrahedrally coordinated molecules combined with the blue shift, which progressively increases the overlap with the donor OH.

It is difficult to quantify the number of water molecules and/or ions in the interfacial region because of the fact that the sum-frequency measurement convolves the number of molecules with their orientations and transition moments. An additional complicating factor is that the transition moments, even for a particular interfacial species (e.g., the donor OH), may change as the anion is changed. OH transition strengths typically decrease as the OH vibration frequencies shift to the blue and typically increase as the frequencies shift to the red.^{12,40,41} Thus, as the tetrahedrally coordinated peak (and to a lesser extent the donor OH) blue shifts, the transition moment is expected to change, increasing for the NaF solution peaks but decreasing for the Cl^- , Br^- , and I^- solutions.

Previous VSFS studies have examined the effects of simple acids such as HCl , HNO_3 , and H_2SO_4 and their corresponding salts at the vapor/water interface.^{16,42,43} These studies concluded that the anions were located closer to the surface than the cations. However, these studies primarily (with the exception of Cl^-) looked at large, highly polarizable, oxygen-containing anions capable of significant hydrogen bonding interactions. These studies were not able to attribute the spectral changes to specific interfacial water species, as has been possible in these isotopic dilution studies.

Overall these studies confirm the presence of anions in the interfacial region. The VSF response from the tetrahedrally coordinated water molecules indicates that F^- enhances the water bonding network in the surface region, whereas Cl^- , Br^- , and I^- cause a weakening of the network. Unlike the tetrahedrally coordinated water peak, the uncoupled donor OH does not exhibit significant spectral changes for any of the salt solutions, unlike bulk studies of the salts in $\text{HOD}/\text{H}_2\text{O}/\text{D}_2\text{O}$ mixtures. This lack of change indicates that there are few ions in the topmost surface layer of the surface region, where the donor OH resides. This does not necessarily imply that there is a top surface layer of pure water but only that the surface concentration of ions is small enough not to have any significant effect on the bonding character. This decrease in the concentration of ions as the surface is approached is consistent with the thermodynamic picture of the interface in which the total interfacial ion concentration is lower than that of the bulk. The presence of the two peaks assigned to ion-solvating water molecules combined with the unchanging nature of the donor

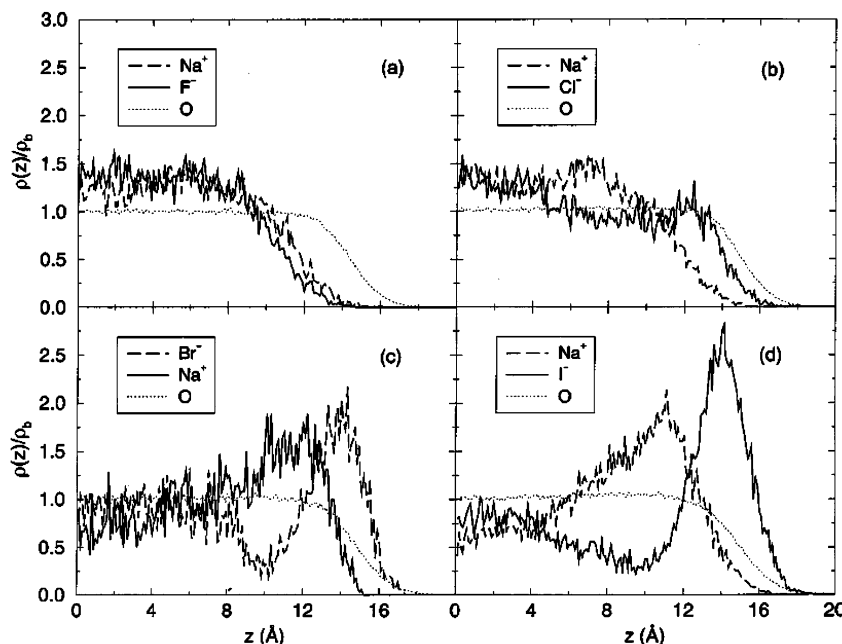


Figure 10. Results of simulations of aqueous salts at the vapor/H₂O interface calculated by Jungwirth and Tobias. The concentration of all four solutions is 1.2 M. Shown are the normalized number density profiles along the distance from the simulation box center for the cation, anion, and water oxygen atoms. The interfacial region defined for these simulations is $|z| > 12.5 \text{ \AA}$. Reprinted with permission from ref. 7, copyright 2002, American Chemical Society.

OH indicates that these solvating molecules are not confined to the top layer of the interfacial region, where there are likely few anions, but rather are dispersed throughout the interfacial region. VSF measurements sample molecules as deeply into the solution as the influence of the interface is felt. A value for this depth is not experimentally obtainable from the VSF measurements. For estimates of the interfacial thickness, it is useful to examine recent molecular dynamics simulations of these salts at the vapor/water interface.

MD Simulations

Molecular dynamics simulations have been performed on a variety of simple ions and salts at the vapor/water interface over the past decade,^{8,44,45} but only recently have relatively concentrated solutions (molar concentrations as opposed to single ions) been studied.^{5–7} Results of MD simulations of 1.2 M aqueous solutions of NaF, NaCl, NaBr, and NaI, performed by Jungwirth and Tobias, are shown in Figure 10. Only the results of the simulations, not the methods, are presented here. Readers are referred to refs 5–7 for further details. The normalized density profiles of the anions, cations, and water oxygen atoms as a function of distance from the center of the box are shown for each of the four salt solutions. These density profiles show that the interfacial region (the region over which an inhomogeneity exists) is much larger for the salt-containing solutions than for neat H₂O. The NaF solution exhibits a steady decrease in both anion and cation concentration from the bulk solution toward the interface, with the concentration of Na⁺ being slightly higher near the surface than that of F⁻. The distribution of ions in the interfacial region in the NaCl, NaBr, and NaI solutions becomes considerably more structured as the anion size increases, with the anions preferentially segregating toward the interface. The NaI solution most clearly shows this distinct separation of the cations and anions near the solution surface.

The simulations also calculate different reorientation effects for the NaF solution than for the NaCl, NaBr, and NaI solutions. The NaF solution interface shows very little reorientation of the H₂O–H₂O bonds relative to neat H₂O, but the H₂O–F⁻

bonds become more perpendicular to the interface. For the NaCl, NaBr, and NaI solution interfaces, the H₂O–H₂O bonds become more perpendicular to the interfacial plane (the effect becomes stronger as the anion size increases). In terms of the contribution to changes in the VSF spectra, the more important orientation effect is that of the H₂O–H₂O bonds, as the calculated numbers of H₂O–anion bonds per water molecule in the interfacial region are quite small: 0.02 for F⁻, 0.07 for Cl⁻, 0.13 for Br⁻, and 0.17 for I⁻.⁶

Such a structure of separated anions and cations combined with the reorientation of water–water hydrogen bonds to be more perpendicular to the interfacial plane should result in a significant enhancement of the sum-frequency signal arising from these salt solutions. The combined effect of a larger number of water molecules with their dipole moments perpendicular to the interfacial plane and an enhancement in the transition strength arising from the electric field between the separated ions should result in a progressively larger signal as the anion size increases. The nearly constant areas of the tetrahedral, donor, and free OH peaks obtained from the experimental spectra indicate that a significant enhancement of this type is not observed. As with MD simulations of the pure vapor/H₂O interface, it is very difficult to compare sum-frequency spectra with density and orientation profiles. With the techniques emerging for calculating sum-frequency spectra from MD simulations,^{46–48} eventually sum-frequency spectra should be able to be calculated from simulations such as those presented here. The calculation of such spectra is a good check for the potentials and polarizabilities used in these simulations because the calculated quantities can then be directly compared to experimentally measured quantities.

Conclusions

These studies have examined the hydrogen bonding of water molecules in the surface region of aqueous sodium halide salt solutions to (1) determine whether there are anions in the surface region and (2) examine the effect of these salts on the hydrogen bonding character of surface water molecules. In these VSF

spectroscopic studies of the OH stretching region, VSFS directly probes the surface region that coincides with the definition of the surface region as defined in the Gibbs treatment (i.e., the region in which the number of molecules of solute per unit volume differs from that of the bulk). For our studies of high ionic strength salts, the double-layer thickness expected from Gouy–Chapman theory is very small, $\sim 2.7 \text{ \AA}$.¹

The isotopic dilution experiments reported herein have allowed a more complete understanding of the presence and effect of ions on the hydrogen bonding of interfacial water molecules in the surface region and at the topmost layer of the water surface. Overall the spectral observations confirm the presence of ions and particularly anions in the interfacial region. Tetrahedrally coordinated water molecules undergo frequency shifts and changes in width that are consistent with those observed in bulk IR and Raman studies of aqueous solutions of these salts. These spectral changes are consistent with the structure-making nature of F^- and the structure-breaking natures of Cl^- , Br^- , and I^- . In contrast, the uncoupled donor OH that resides in the topmost portion of the surface region does not exhibit significant spectral changes for any of the salt solutions, unlike bulk studies of the salts in $\text{HOD}/\text{H}_2\text{O}/\text{D}_2\text{O}$ mixtures. This indicates that ions in the topmost layer do not cause a measurable change in the hydrogen bonding between these boundary water molecules. This decrease in the concentration of ions as the surface is approached is consistent with the thermodynamic picture of the interface, in which the total interfacial ion concentration is lower than that of the bulk. The nearly constant areas of the tetrahedral, donor, and free OH peaks obtained from the experimental spectra indicate that a significant enhancement in anion concentration in the surface region that is predicted from MD simulations is not present. The VSF spectra also show no evidence of the distinct, separated anion–cation structures at the interface of the NaBr and NaI solutions, calculated by MD simulations. Direct comparison of the experimental SF spectra with SF spectra calculated from MD simulations may provide insight into the source of these differences.

Acknowledgment. We thank the National Science Foundation (CHE 0243856) for supporting this research and the Office of Naval Research for instrumentation. E.A.R. also acknowledges the support of the NSF IGERT program at the University of Oregon. We also acknowledge our valued and delightful discussions with Professor Brian Pethica on topics related to this paper.

References and Notes

- (1) Chatteraj, D. K.; Birdi, K. S. *Adsorption and the Gibbs Surface Excess*; Plenum Press: New York, 1984.
- (2) Ghosal, S.; Shbeeb, A.; Hemminger, J. C. *Geophys. Res. Lett.* **2000**, 27, 1879.
- (3) Hu, J. H.; Shi, Q.; Davidovits, P.; Worsnop, D. R.; Zahniser, M. S.; Kolb, C. E. *J. Phys. Chem.* **1995**, 99, 8768.
- (4) Knipping, E. M.; Lakin, M. J.; Foster, K. L.; Jungwirth, P.; Tobias, D. J.; Gerber, R. B.; Dabdub, D.; Finlayson-Pitts, B. J. *Science* **2000**, 288, 301.
- (5) Jungwirth, P.; Tobias, D. J. *J. Phys. Chem. B* **2000**, 104, 7702.
- (6) Jungwirth, P.; Tobias, D. J. *J. Phys. Chem. B* **2001**, 105, 10468.
- (7) Jungwirth, P.; Tobias, D. J. *J. Phys. Chem. B* **2002**, 106, 6361.
- (8) Dang, L. X. *J. Phys. Chem. B* **2002**, 106, 10388.
- (9) Kolb, C. E. *Nature* **2002**, 417, 597.
- (10) Finlayson-Pitts, B. J.; Pitts, J. N., Jr. *Chemistry of the Upper and Lower Atmosphere*; Academic Press: San Diego, CA, 2000.
- (11) Demou, E.; Donaldson, D. J. *J. Phys. Chem. A* **2002**, 106, 982.
- (12) *Aqueous Solutions of Simple Electrolytes*; Franks, F., Ed.; Plenum Press: New York, 1973; Vol. 3.
- (13) Cacace, M. G.; Landau, E. M.; Ramsden, J. J. *Q. Rev. Biophys.* **1997**, 30, 241.
- (14) Richmond, G. L. *Chem. Rev.* **2002**, 102, 2693.
- (15) Miranda, P. B.; Shen, Y. R. *J. Phys. Chem. B* **1999**, 103, 3292.
- (16) Shultz, M. J.; Baldelli, S.; Schnitzer, C.; Simonelli, D. *J. Phys. Chem. B* **2002**, 106, 5313.
- (17) Raymond, E. A.; Tarbuck, T. L.; Richmond, G. L. *J. Phys. Chem. B* **2002**, 106, 2817.
- (18) Raymond, E. A.; Tarbuck, T. L.; Brown, M. G.; Richmond, G. L. *J. Phys. Chem. B* **2003**, 107, 546.
- (19) Scatena, L. F.; Brown, M. G.; Richmond, G. L. *Science* **2001**, 292, 908.
- (20) Onsager, L.; Samaras, N. N. T. *J. Chem. Phys.* **1934**, 2, 528.
- (21) Wagner, C. *Phys. Z.* **1924**, 25, 474.
- (22) Matubayasi, N.; Tsunetomo, K.; Sato, I.; Akizuki, R.; Morishita, T.; Matuzawa, A.; Natsukari, Y. *J. Colloid Interface Sci.* **2001**, 243, 444.
- (23) Jarvis, N. L.; Scheiman, M. A. *J. Phys. Chem.* **1968**, 72, 74.
- (24) Markin, V. S.; Volkov, A. G. *J. Phys. Chem. B* **2002**, 106, 11810.
- (25) Bain, C. D. *J. Chem. Soc., Faraday Trans.* **1995**, 91, 1281.
- (26) Richmond, G. L. *Annu. Rev. Phys. Chem.* **2001**, 52, 357.
- (27) Allen, H. C.; Raymond, E. A.; Richmond, G. L. *J. Phys. Chem. A* **2001**, 105, 1649.
- (28) Gragson, D. E.; McCarty, B. M.; Richmond, G. L.; Alavi, D. S. *J. Opt. Soc. Am. B* **1996**, 13, 2075.
- (29) Brown, M. G.; Raymond, E. A.; Allen, H. C.; Scatena, L. F.; Richmond, G. L. *J. Phys. Chem. A* **2000**, 104, 10220.
- (30) Hirose, C.; Akamatsu, N.; Domen, K. *Appl. Spectrosc.* **1992**, 46, 1051.
- (31) Hirose, C.; Akamatsu, N.; Domen, K. *J. Chem. Phys.* **1992**, 96, 997.
- (32) Terpstra, P.; Combes, D.; Zwick, A. *J. Chem. Phys.* **1990**, 92, 65.
- (33) Rull, F.; de Saja, J. A. *J. Raman Spectrosc.* **1986**, 17, 167.
- (34) Abe, N.; Ito, M. *J. Raman Spectrosc.* **1978**, 7, 161.
- (35) Kropman, M. F.; Bakker, H. J. *J. Chem. Phys.* **2001**, 115, 8942.
- (36) Ayotte, P.; Weddle, G. H.; Kim, J.; Johnson, M. A. *J. Am. Chem. Soc.* **1998**, 120, 12361.
- (37) Ayotte, P.; Weddle, G. H.; Johnson, M. A. *J. Chem. Phys.* **1999**, 110, 7129.
- (38) Scatena, L. F.; Richmond, G. L. *Chem. Phys. Lett.* **2004**, 383, 491.
- (39) Robertson, W. H.; Johnson, M. A. *Annu. Rev. Phys. Chem.* **2003**, 54, 173.
- (40) *The Physics and Physical Chemistry of Water*; Franks, F., Ed.; Plenum Press: New York, 1972; Vol. 1.
- (41) Walrafen, G. E. *Raman and Infrared Spectral Investigations of Water Structure. In Water: A Comprehensive Treatise*; Franks, F., Ed.; Plenum Press: New York, 1972; Vol. 1, Chapter 5.
- (42) Shultz, M. J.; Schnitzer, C.; Simonelli, D.; Baldelli, S. *Int. Rev. Phys. Chem.* **2000**, 19, 123.
- (43) Schnitzer, C.; Baldelli, S.; Shultz, M. J. *J. Phys. Chem. B* **2000**, 104, 585.
- (44) Wilson, M. A.; Pohorille, A. *J. Chem. Phys.* **1991**, 95, 6005.
- (45) Benjamin, I. *J. Chem. Phys.* **1991**, 95, 3698.
- (46) Perry, A.; Alhribi, H.; Space, B. *J. Chem. Phys.* **2003**, 118, 8411.
- (47) Morita, A.; Hynes, J. T. *Chem. Phys.* **2000**, 258, 371.
- (48) Morita, A.; Hynes, J. T. *J. Phys. Chem. B* **2002**, 106, 673.